*Steel and Composite Structures, Vol. 3, No. 6 (2003) 451-474*
DOI: http://dx.doi.org/10.12989/scs.2003.3.6.451 

# Serviceability design of a cold-formed steel portal frame having semi-rigid joints

J.B.P. Lim†

*The Steel Construction Institute, Silwood Park, Ascot, Berkshire SL5 7QN, UK*

D.A. Nethercot‡

*Imperial College, London, UK*

*(Received July 24, 2003, Accepted December 10, 2003)*

**Abstract.** Details are given of a cold-formed steel portal framing system that uses simple bolted moment-connections for both the eaves and apex joints. However, such joints function as semi-rigid and, as a result, the design of the proposed system will be dominated by serviceability requirements. While serviceability is a mandatory design requirement, actual deflection limits for portal frames are not prescribed in many of the national standards. In this paper, a review of the design constraints that have an effect on deflection limits is discussed, and rational values appropriate for use with cold-formed steel portal frames are recommended. Adopting these deflection limits, it is shown through a design example how a cold-formed steel portal frame having semi-rigid eaves and apex joints can be a feasible alternative to rigid-jointed frames in appropriate circumstances.

**Key words:** cold-formed steel portal frames; deflection limits; finite connection-length; semi-rigid joints; serviceability requirements.

## 1. Introduction

Portal frames account for some 40% of the constructional steel used in the UK, the vast majority of these are fabricated from hot-rolled steel sections. Using hot-rolled steel, portal frames with spans of up to 60 m may be constructed. However, for portal frames with more modest spans (around 12 m), as found in low-rise commercial, light industrial and agricultural buildings, it may be more cost-effective to use lighter cold-formed steel sections instead of hot-rolled steel as the primary load-carrying members.

The design of portal frames is heavily influenced by serviceability requirements. For this reason, hot-rolled steel portal frames are conventionally designed using rigid joints to reduce frame deflections. With cold-formed steel portal frames, with flexible column and rafter members, designers have assumed that the use of rigid joints is equally important.

However, joints suitable for use with relatively thin cold-formed sections that function as rigid are expensive both to fabricate and to assemble on site. Rigid joints are therefore not usually found in cold-formed steel construction; in this paper, various methods described in the literature for the fabrication of

†Engineer
‡Professor

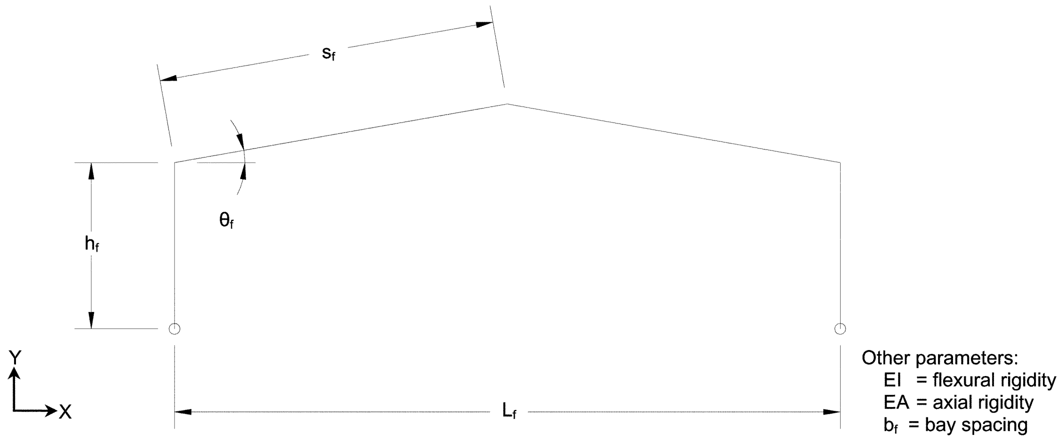


Fig. 1 Portal frame parameters

rigid joints are described. On the other hand, cold-formed steel joints that function as semi-rigid can be formed easily through brackets, and such joints are also easy to assemble on site.

Serviceability requirements may thus be expected to control the feasibility of using a cold-formed steel portal frame having semi-rigid joints. However, while serviceability is a mandatory design requirement, deflection limits for portal frames are not specified in many national standards. The decision on whether a portal frame satisfies serviceability requirements is therefore left to the judgement of an engineer. If the deflection limits suggested by an engineer are too stringent, the portal frame will be unnecessarily expensive. On the other hand, if the deflection limits are too generous, there will be implications later on for the cladding, water-tightness and visual acceptability of the building.

In this paper, a literature review of the design requirements that have an effect on deflection limits is discussed, and rational deflection limits appropriate for use with cold-formed steel portal frames are recommended. Using these deflection limits, the feasibility of a cold-formed steel portal frame having semi-rigid eaves and apex joints is investigated.

The parameters that have a bearing on the portal frame deflection limits are shown in Fig. 1. These parameters are as follows: span of frame $L_f$, height to eaves $h_f$, length of rafter $s_f$, pitch of frame $\theta_f$, flexural rigidity of members EI, axial rigidity of members EA and bay spacing $b_f$.

## 2. Rigid-jointed cold-formed steel portal frames

The use of cold-formed steel sections as the primary load-carrying members in frames of modest span can have a number of advantages over the use of hot-rolled steel sections. To begin with, bolt-holes need not be drilled but instead are automatically precision punched during the rolling of the sections. Maintenance-free pre-galvanised cold-formed steel sections can be used for the column and rafter members and so painting to prevent rusting is not required. Transportation costs are reduced due to efficient stacking of the cold-formed steel members. Acquisition costs are reduced as the secondary members can also be purchased from the same manufacturer. Smaller foundations can also be used with cold-formed steel portal frames. Finally an on-site crane is not always required as the frame may be erected manually by a few semi-skilled workers.

Several methods for fabricating rigid-joints for use as the eaves and apex joints in cold-formed steel

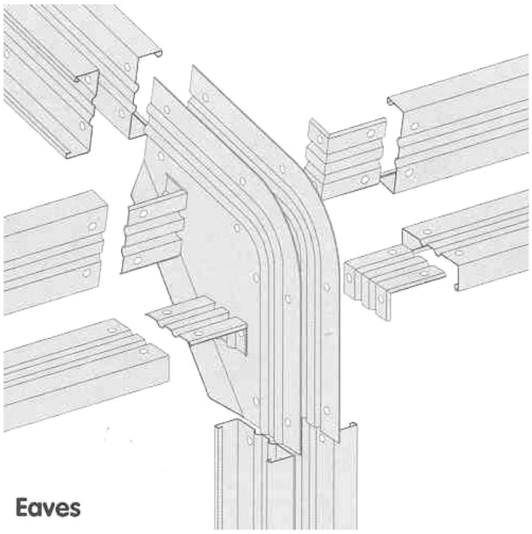


Fig. 2 Details of the eaves joint of the Swagebeam (courtesy of Ayrshire)

portal frames are available. Of these, the most successful, and also the most innovative, is that used for the Swagebeam portal framing system (Kirk 1986). Fig. 2 shows details of the eaves joint of the Swagebeam system. As can be seen, the eaves joint is formed through back-to-back brackets to which the webs of the channel-sections used for both the column and rafter members are bolted. The novelty of the joint is in the swages found in both the brackets and the column and rafter members. Therefore, when the joint resists a moment, the swages on both the bracket and the swaged channel-section interlock. Swage interlock provides the joints of the Swagebeam portal framing system with two unique advantages over alterative joint arrangements. Firstly, fewer bolts are required to form each joint. As erection costs are one of the most important concerns in all forms of steel construction, a joint that requires few bolts has a significant advantage over alternative joint arrangements. Secondly, the interlocking of the joints means that the frame can be designed with the assumption that the joints are rigid and do not slip under load.

Baigent and Hancock (1986) tested a cold-formed steel portal frame in which rigid eaves and apex joints were formed through bolting the cold-formed steel channel-sections, used for the column and rafter members, to stiffened plates with 19 mm high-tensile friction-grip bolts.

De Vos and Van Rensburg (1997) proposed a cold-formed steel portal frame using column and rafter members comprised of welding C-sections to form a rectangular hollow section. Rigid eaves and apex joints would be formed by on-site welding.

Masika and Dunai (1995) tested the eaves joint of a cold-formed steel portal frame. The arrangement of the eaves joint was similar to that of a hot-rolled steel portal frame with a haunched rafter to which an end plate was welded.

With the exception of the Swagebeam joints, all the joints described in the literature have the disadvantage of not being appropriate for use with galvanised steel. For example, Baigent required high-tensile friction-grip bolts to form the eaves and apex joints; such high-tensile friction-grip bolts are not particularly effective when used with galvanised steel due to the low coefficient of friction of the galvanised surface. On the other hand, the joints suggested by both De Vos and Masika require welding, which is not recommended for galvanised steel owing to the ensuing emissions of poisonous gasses and destruction of the galvanised layer. As explained previously, the use of galvanised steel is one of the most important attractions of cold-formed steel construction.

The Swagebeam joint is therefore the most feasible method of fabricating rigid joints for cold-formed steel portal frames. However, its limitation is the manufacturing costs. The Swagebeam is not a standard section and so requires specialist tooling to produce; at present, there are only three sizes of Swagebeam sections available. Moreover, the machinery required to press swages into the brackets is both expensive and not easily available.

## 3. Description of proposed semi-rigid joint

Fig. 3 and Fig. 4 show details of the semi-rigid eaves and apex joints proposed for use with a cold-

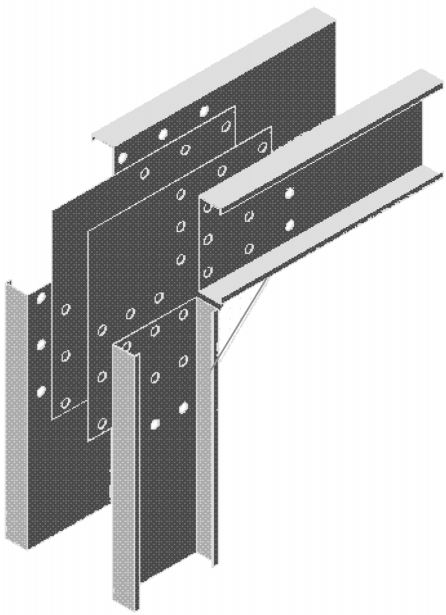

Fig. 3 Details of the proposed arrangement for the eaves joint

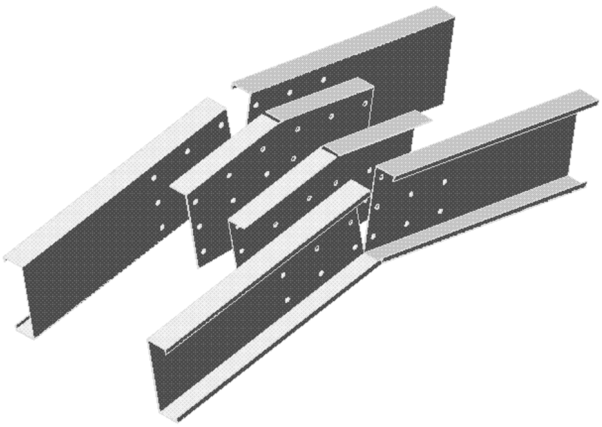

Fig. 4 Details of the proposed arrangement for the apex joint

formed steel portal framing system. Each moment connection is formed through brackets bolted between the webs of back-to-back channel-sections used as the column and rafter members. The advantage over the Swagebeam joints is that any size of channel-section can be used. The semi-rigidity of the joints is principally due to the elongation of the bolt-holes in both the brackets and channel-sections.

## 4. Serviceability requirements

Mandatory deflection limits for portal frames are not normally found in national codes of practice. A typical explanation for this specific exclusion is that the deflections of portal frames have no direct significance on the serviceability of the portal frame itself. Although this explanation is technically correct, excessive deflections will affect, among other things, the serviceability of the cladding of the frame, water tightness and the visual acceptability of the building in general. It is argued, therefore, that the implications of excessive frame deflections depend on the type of cladding and other constructional details and so should be outside the scope of the code. Guidance from BS5950: Part1, which is typical of that provided in many codes, is thus limited to the general statement regarding deflections given in Clause 2.5.1: “The deflection under serviceability loads of a building or part should not impair the strength or efficiency of the structure or its components or cause damage to the finishings.”

### *4.1. Considerations for deflection limits*

The typical use of cold-formed steel portal frames is limited to light industrial buildings without gantry cranes and suspended ceilings. There are therefore only three main considerations for deflection limits:

(a) The absolute horizontal eaves deflection due to live load should not cause damage to the cladding, fixings or brickwork.

(b) The differential horizontal eaves deflection between the gable frame (which is effectively rigid owing to stiffening provided by wall sheeting and internal gable columns) and its adjacent frame should not be excessive. If the differential horizontal deflection is too great, significant stressed skin action will develop which, if not properly accounted for in the design of the fixings, may result in the fixings becoming overstrained, in turn leading to localised hole elongation and tearing of sheeting. Such damage may result in leakage of water into the building. In addition, differential horizontal deflection at the eaves should be visually acceptable.

(c) Similarly, any differential vertical apex deflection between the gable frame and its adjacent frame should also be visually acceptable and should not lead to ponding of water.

### *4.2. Guidance found in the literature*

Woolcock and Kitipornchai (1986) published the results of a survey in which experienced designers were questioned on their views on deflection limits. Suggestions for deflection limits for both industrial buildings and farm sheds were given; the term cold-formed steel, however, was not mentioned specifically. Table 1 shows the deflection limits for industrial buildings. For lateral spread at the eaves, but not for apex deflection, various types of industrial building were considered. The values shown in Table 1 for the lateral spread at the eaves are for an industrial building with steel clad walls but without gantry cranes, suspended ceilings and internal partitions (against external walls or columns). Reference was made to the fact that pre-camber or pre-set may be employed but it was assumed that such

Table 1 Deflection limits suggested by Woolcock and Kitipornchai

| Deflection category | Absolute/relative deflection | Type of load | Deflection limit |
|---|---|---|---|
| Lateral eaves deflection | Absolute | Dead load + Live load | $h_f$ / 150 |
| | Relative | Dead load + Live load | $b_f$ / 200 |
| Vertical apex deflection | Absolute | Dead load | $L_f$ / 360 |
| | Absolute | Dead load + Live load | $L_f$ / 240 |
| | Absolute | Dead load + Wind load | $L_f$ / 240 |

Table 2 Deflection limits suggested by the SCI for portal frames under both live and wind loads

| Deflection category | Reason for limit | Absolute/relative deflection | Deflection limit |
|---|---|---|---|
| Lateral eaves deflection | Damage to side cladding | Absolute | $h_f$ / 100 |
| | Damage to roof cladding | Relative | $b_f$ / 200 |
| Vertical apex deflection | Ponding of water | Relative | Minimum of $b_f$ / 100 and $\sqrt{b_f^2 + s_f^2}/125$ |

techniques are not always used.

The Steel Construction Institute (SCI) has also produced a document in which suggestions were made for deflection limits (SCI Advisory Desk 1991). Unlike the survey by Woolcock and Kitipornchai, however, deflection limits for live and wind load cases only were given as it was assumed that dead load effects should be compensated by the initial pre-camber of the portal frame. Moreover, the deflection limits suggested by the SCI did not make a distinction for the type of portal frame, nor its use, but defined the deflection limits on the basis of the effect that excessive deflection would have on the cladding of the frame. Different deflection limits were given for different types of cladding. Table 2 shows the deflection limits suggested for frames that use profiled metal cladding for the sides and roofs.

### *4.3. Recommended deflection limits*

Guidelines found in the literature for deflection limits for portal frames were discussed in the previous Section. While these guidelines are useful, it should be remembered that they are intended more for use with hot-rolled steel portal frames which have a greater variety of uses than the simple cold-formed steel portal frames considered here; gantry cranes, suspended ceilings and internal partitions may have been taken into account when the suggested limits were chosen. Moreover, unlike cold-formed steel portal frames of similar spans, the height to eaves of hot-rolled steel portal frames is much greater. Spans of up to 50 m and heights of up to 15 m are not uncommon with hot-rolled steel portal frames; high frames have implications with respect to the deflection limits in the code for frame stability and so may also have had an influence on the selection of the deflection limits found in the literature.

Table 3 shows the deflection limits suggested by the Authors for use with cold-formed steel frames. A distinction between the classification of deflection limits into absolute or relative is not made as such a distinction is only necessary if the bay spacings are not equal, and deflections of each frame therefore different. It is also assumed that pre-cambering or pre-setting techniques have been used.

The deflection limits for lateral spread have been divided into the same categories as given by the SCI so that a distinction may be made between them: a value for the side cladding and one for the roof cladding. The deflection limit of $h_f$/ 100 for absolute deflection of the side cladding has been taken

Table 3 Deflection limits suggested by the Authors for cold-formed steel portal frames under both live and wind loads

| Deflection category | Reason for limit | Deflection limit |
|---|---|---|
| Lateral eaves deflection | Damage to side cladding | $h_f$ / 100 |
| | Damage to roof cladding | $h_f$ / 150 |
| Vertical apex deflection | Ponding of water | $\sqrt{b_f^2 + s_f^2}/125$ |
| | Visual acceptability | $L_f$ / 240 |

from the SCI document. A lateral deflection limit for roof cladding of $h_f$ /150 has, however, been used instead of $b_f$ /200 because this reflects the recommendation to be made in a forthcoming document to be published on portal frame deflections by the Australian Institute of Steel Construction (AISC). The deflection limit of $b_f$ /200 was taken from the current AISC document on portal frame deflections.

For the apex deflection it can be seen that a deflection limit for ponding of water of $\sqrt{(b_f^2 + s_f^2)}/125$ has been used; the limit of $b_f$/100 also suggested by the SCI has not been used as there would appear to be no logical reason for another limit based solely on $b_f$. Instead, the apex deflection limit of $L_f$ /240 suggested by Woodcock and Kitipornchai has been adopted for the visual acceptability of frames due to the sagging of the rafters. A similar deflection limit for the visual acceptablity of the frame due to lateral spread at the eaves is not necessary as the lateral spread at the eaves is much smaller than the apex deflection.

## 5. Design loads

### 5.1. Standard frame

Details of the standard frame are shown in Fig. 5; the dimensions of the back-to-back channel-sections used for both the column and rafter of the portal frame are shown in Fig. 6. The moment-capacity of the back-to-back channel-sections calculated using BS5950: Part 5 (1998), and assuming a yield stress of steel of 280 N/mm$^2$, is 82.8 kN.m. The bay spacing is to be determined. The standard frame will be designed using both rigid and semi-rigid joints

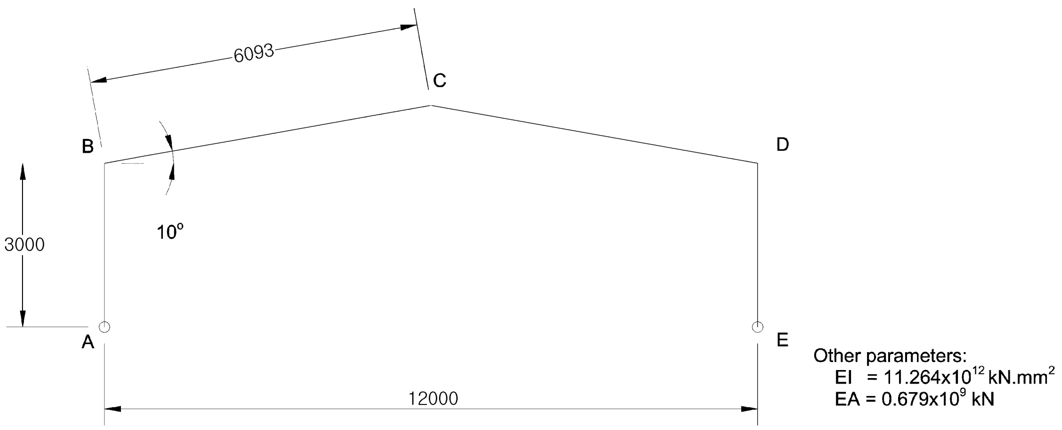


Fig. 5 Details of standard portal frame used in study

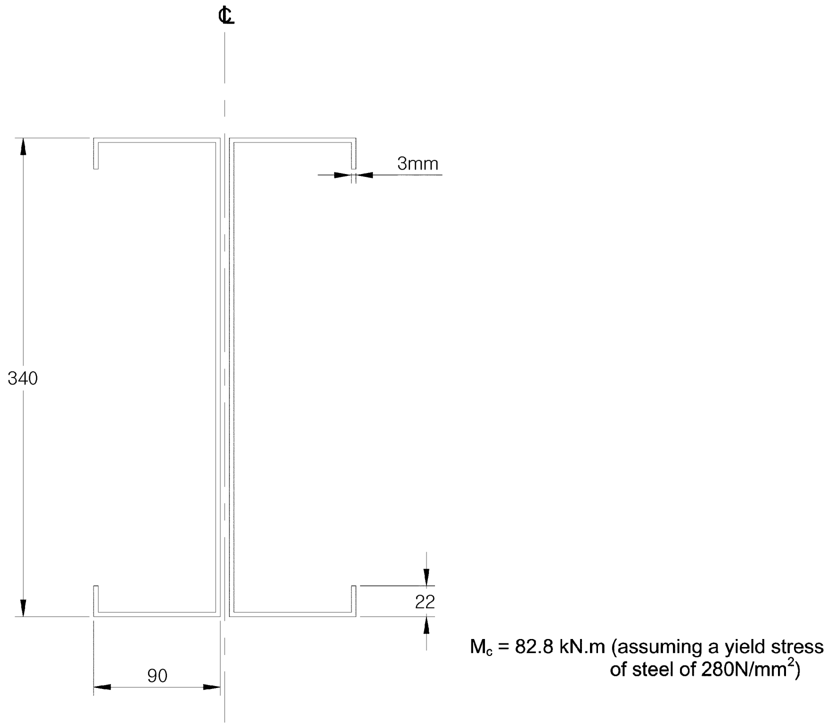


Fig. 6 Dimensions of back-to-back channel-section used for column and rafter members

### *5.2. Dead and live loads*

The dead and live loads that will be applied to the frame are as follows:

| | |
|---|---|
| dead load due to self-weight of frame (DL) | 0.27 kN/m |
| dead load due to cladding (DL) | 0.09 kN/m$^2$ |
| live load due to snow and services (LL) | 0.75 kN/m$^2$ |

### *5.3. Wind load*

From the British Standard Code of practice on wind loading for the design of buildings CP3(1972)[3], the wind load pressure $q$ is calculated from a design wind speed $V_s$, which in turn is calculated from a basic wind speed $V$ multiplied by factors $S_1$ and $S_2$ and $S_3$. A basic wind speed of 46 m/s will be assumed as this is the average basic wind speed for the U.K., and factors $S_1$ and $S_3$ will be taken as 1.0 and factor $S_2$ as 0.65. Therefore the design wind speed

$$V_s = S_1 S_2 S_3 V = 29.9 \text{ m/s}$$

and the wind load pressure

[3] The authors are aware that CP3 has been superseded by BS 6399: Part 2. However, this should make little difference to the conclusions drawn in this Paper, and the trends high-lighted, as no actual buildings are considered.

Table 4 Coefficients of external pressure $C_{pe}$

| Description | Coefficient $C_{pe}$ on face | | | |
|---|---|---|---|---|
| | AB | BC | CD | DE |
| Wind acting on side of frame | 0.7 | -1.2 | -0.4 | -0.25 |
| Wind acting on end of frame | -0.5 | -0.6 | -0.6 | -0.5 |

Table 5 Coefficients of pressure corresponding to different wind load cases

| Wind load combination | Description | Coefficient on face | | | |
|---|---|---|---|---|---|
| | | AB | BC | CD | DE |
| WLC1 | Wind on side + internal pressure | 0.5 | -1.4 | -0.6 | -0.45 |
| WLC2 | Wind on side + internal suction | 1.0 | -0.9 | -0.1 | 0.05 |
| WLC3 | Wind on end + internal pressure | -0.7 | -0.8 | -0.8 | -0.7 |
| WLC4 | Wind on end + internal suction | -0.2 | -0.3 | -0.3 | -0.2 |

$$q = 0.613\ V_s^2 = 548.0\ \text{N/m}^2 = 0.55\ \text{kN/m}^2$$

The pressure acting on each of the four faces of the frame (AB, BC, CD and DE) is obtained by multiplying $q$ by a coefficient of pressure. The coefficient of pressure acting on each face is obtained from a combination of the external pressure coefficient $C_{pe}$ and the internal pressure coefficient $C_{pi}$. There are two separate cases of both $C_{pe}$ and $C_{pi}$, and, therefore four possible combinations of $C_{pe}$ and $C_{pi}$, which result in four wind load combinations (WLC1 to WLC4).

From CP3, for the frame shown in Fig. 5, $C_{pe}$ should be calculated for wind acting on the side and on the end. These values of $C_{pe}$ are shown in Table 4.

From Appendix E of CP3, for buildings of normal permeability, $C_{pi}$ has a minimum value of -0.2 for pressure, and a maximum value of 0.3 for suction.

The four wind load combinations (WLC1 to WLC4), and their corresponding coefficients, are shown in Table 5.

It is usually sufficient to consider only wind load combination 1 (WLC1) (Morris and Plum 1988); the coefficient of pressure given by WLC1 are shown in Fig. 7.

### *5.4. Limit state design*

The frame will be checked at the ultimate limit state for the following two ultimate load combinations:

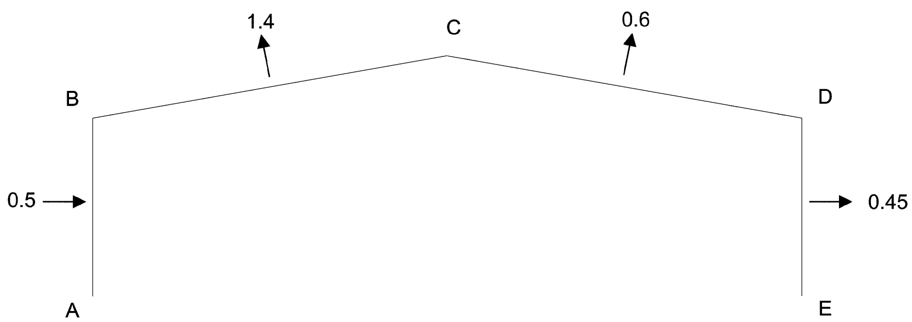


Fig. 7 Coefficients of wind pressure for wind load combination 1 (WLC1)

ULC1 = 1.4 × DL + 1.6 × LL
ULC2 = 1.0 × DL + 1.4 × WLC1

The frame will also be checked at the serviceability limit state for the following two serviceability load combinations:

SLC1 = 1.0 × LL
SLC2 = 1.0 × WLC1

## 6. Frame design using rigid joints

The standard portal frame shown in Fig. 5 will be analysed assuming rigid joints. From the results of this frame analysis, a suitable bay spacing will be selected and the eaves and apex deflections at serviceability live loads compared against the recommendations made in Table 1.

### 6.1. Beam idealisation of frame

The general purpose finite element program ANSYS will be used for the frame analysis (ANSYS 1998). Fig. 8 shows the beam idealisation that will be employed. BEAM3, a 2-D elastic beam element, is used for both the column and rafter members. For these members the gross section properties of the Valleybeam are used, as the purpose of the analysis is to determine the initial stiffness of the frame. If the effective section properties of the Valleybeam were used, as calculated from BS5950: Part 5, the section properties would represent those at failure of the sections.

### 6.2. Frame analysis

Fig. 9 shows the deflected shape and bending moment diagram of the portal frame when loaded vertically by a uniformly distributed load of 1 kN/m.

Fig. 10 shows the deflected shape and bending moment diagram of the portal frame under uniformly distributed load that corresponds to the coefficients of pressure shown in Fig. 7 for wind load combination 1 (WLC1).

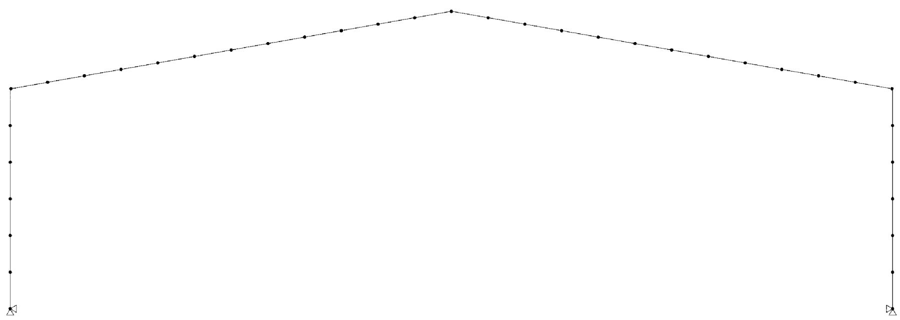

Fig. 8 Details of beam model

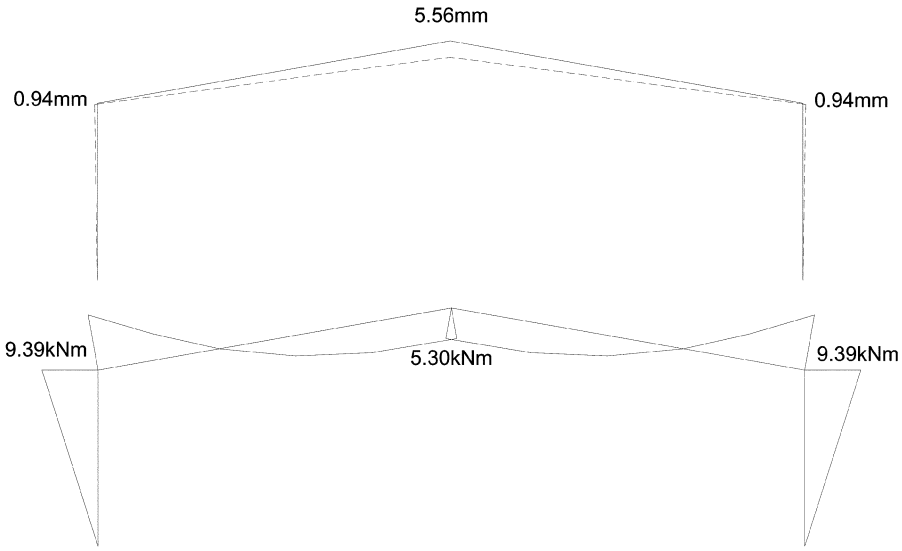


Fig. 9 Deflected shape and bending moment diagram of rigid-jointed portal frame under 1 kN/m uniformly distributed vertical load

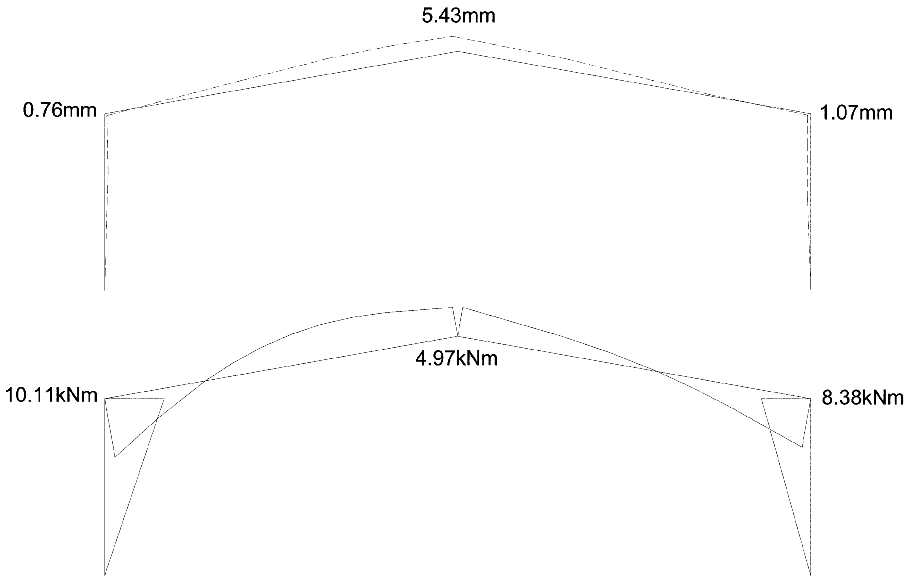


Fig. 10 Deflected shape and bending moment diagram of rigid-jointed portal frame under uniformly distributed load corresponding to the coefficients of pressure for wind load combination 1 (WLC1)

## *6.3. Selection of bay spacing*

The minimum weight solution for a portal frame building that uses a given size of section for the column and rafter members will be the one for which the bay spacing is a maximum and for which both the ultimate and serviceability limit states are satisfied. As with standard design practice, the bay spacing will be determined first on the basis of the ultimate limit state and then checked against the serviceability limit state. It should be noted that only when the bay spacing is known can the live load (and dead load due to cladding) acting on the frame be determined.

To determine the maximum load that can be sustained by each bay of the portal frame, elastic design methods will be used.

### 6.3.1. Ultimate limit state design

As can be seen from Fig. 9, the maximum bending moment under 1 kN/m uniformly distributed vertical load occurs at the eaves of the frame and is 9.39 kN.m. From sub-section 5.1, the moment-capacity of the back-to-back channel-sections is 82.8 kN.m. For ULC1, applying the load factors of 1.4 and 1.6 for dead and live load, repectively, and using the same values of dead and live loads adopted in Section 5, the bay spacing $b_f$ can be calculated from the following expression.

$$(1.4 \times 0.27 \times 9.39) + (1.4 \times 0.09 \times 9.39 \times b_f) + (1.6 \times 0.75 \times 9.39 \times b_f) = 82.8$$

The bay spacing for ULC1 is therefore

$$b_f = 6.37 \text{ m}$$

Following a similar procedure for ULC2 it can be seen from Fig. 10 that the maximum bending moment occurs at the left-hand (windward) side eaves and is 10.11 kN.m. Applying the load factors of 1.0 and 1.4 for dead and wind load, respectively, and using the same values of dead and live loads adopted in Section 5, the bay spacing can be calculated from the following expression

$$(1.0 \times 0.27 \times 9.39) + (1.0 \times 0.09 \times 9.39 \times b_f) - (1.4 \times 0.55 \times 10.11 \times b_f) = -82.8$$

The bay spacing under ULC2 is therefore given by

$$b_f = 12.30 \text{ m}$$

As the bay spacing calculated for ULC1 is less than that for ULC2, the bay spacing for ULC1 is the critical case. For such a bay spacing, the live load ($LL$) acting on the frame is

$$LL = 0.75 \times b_f = 4.78 \text{ kN/m}$$

### 6.3.2. Serviceability limit state

For the bay spacing calculated, the deflections under both serviceability load combination 1 (SLC1) and serviceability load combination 2 (SLC2) are shown in Table 6. As can be seen, for both SLC1 and SLC2, the calculated deflections are well within the limits suggested in Table 3 for cold-formed steel

Table 6 Comparison of calculated serviceability deflections with suggested limits for standard frame having $b_f$ = 6.37 m

| Deflection category | Deflection limit | Deflection limit for frame (mm) | Calculated deflection for frame under SLC1 (mm) | Calculated deflection for frame under SLC2 (mm) |
|---|---|---|---|---|
| Lateral eaves deflection | $h_f / 100$ | 30.0 | 4.5 | 3.8 |
| | $h_f / 150$ | 20.0 | | |
| Vertical apex deflection | $\sqrt{b_f^2 + s_f^2}/125$ | 50.0 | 26.6 | 19.0 |
| | $L_f / 240$ | 70.0 | | |

Note: The deflections shown above for SLC1 and SLC2 are in opposite directions portal frames. No reduction in bay spacing is therefore required and the design of the portal frame assuming rigid joints is therefore controlled by the ultimate limit state.

The deflection at the eaves and apex under SLC1 is therefore $b_f \times LL$ larger than that shown in Fig. 9. Similarly, the deflection at the eaves and apex under SLC2 is therefore $b_f \times q$ larger than that shown in Fig. 10.

## 7. Frame design using semi-rigid joints

The standard portal frame will be designed for the two sets of semi-rigid joints shown in Fig. 11; the corresponding frames are designated as Frame A and Frame B.

Unlike the rigid jointed frame, Frames A and B will not be designed to the ultimate limit state. This is because redistribution of the bending moments under ULC1 and ULC2 will result in both Frames A and B having different ultimate loads, and therefore a different serviceability load.

Instead, the eaves and apex deflections will be checked against the recommendations in Table 1 at the serviceability live load for a bay spacing of 6.37 m.

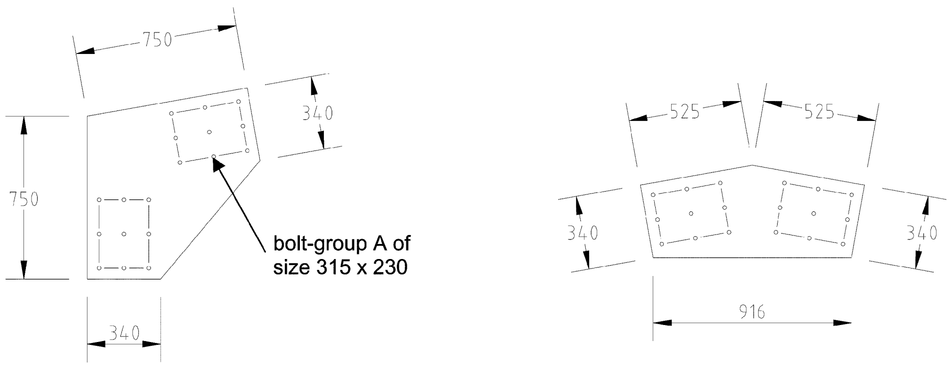


(a) Frame A

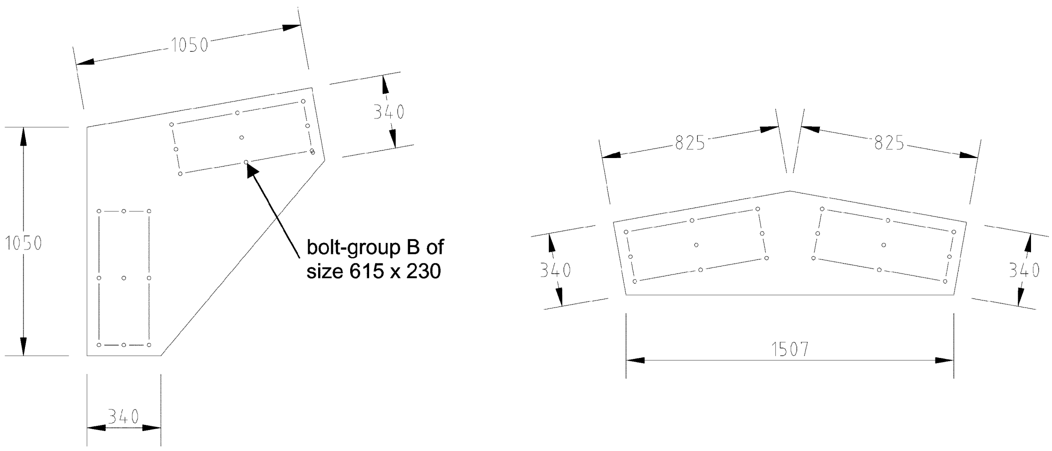


(b) Frame B

Fig. 11 Details of bolt-groups and corresponding sizes of eaves and apex brackets

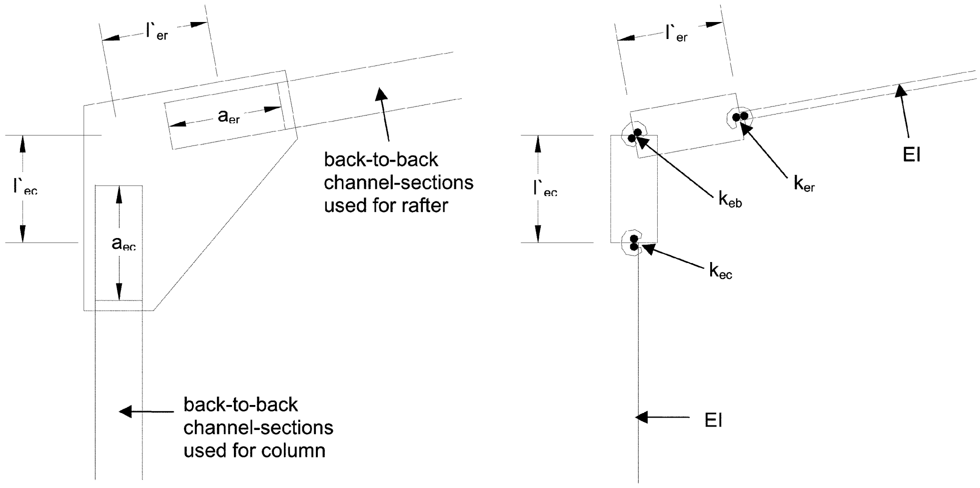


Fig. 12. Beam idealisation of eaves joint

### *7.1. Beam idealisation of frame*

Fig. 12 shows details of the beam idealisation of the eaves joint. As can be seen, the column and rafter members are each connected at the eaves joint through rotational spring elements of stiffness $k_{ec}$ and $k_{er}$, respectively. Each rotational spring is of zero size and connects two coincident nodes, with one node belonging to the member and the other node to the eaves bracket.

As mentioned previously, the semi-rigidity of the joints is due to elongation of the bolt-holes caused by the shear load transmitted by the bolts. A bolt-hole of diameter 18 mm drilled in a 3 mm thick plate (that has an ultimate stress of 280 N/mm$^2$) and bearing against a fully threaded bolt of diameter 16 mm can be shown to have a bolt-hole elongation stiffness $k_b$ of 10.58 kN/mm (Lim 2001, Chung and Ip 2000).

The values of $k_{ec}$ and $k_{er}$ for the spring elements depends on the length and breadth of the bolt-group, the number of bolts used, and the bolt-hole elongation stiffness $k_b$. For connections to the eaves bracket formed by nine bolts, it can be shown that

$$k_{er} = 3/2(a_{er}^2 + b_{er}^2)k_b$$

and

$$k_{ec} = 3/2(a_{ec}^2 + b_{ec}^2)k_b$$

Appropriate formulae for the bolt-group rotational stiffness $k_B$ for various arrays of bolts are shown in Table 7. The length and breadth of the bolt-group are defined as $a_B$ and $b_B$ respectively. It is interesting to note that $k_B$ is proportional to the square of the diagonal length of the bolt-group and that the constant of proportionality depends on the number of bolts in the bolt-group; $k_B$ therefore depends only on the geometry of the bolt-group for a given bolt-hole elongation stiffness $k_b$.

It can also be seen in Fig. 12 that the centre of rotation of each connection (or bolt-group) is not located at the intersection of the centre-lines of the members. This finite connection-length of the joints is idealised using two rigid beam elements. The column and rafter connections at the eaves therefore have finite connection-lengths of $l'_{ec}$ and $l'_{er}$, respectively.

The apex joint is idealised in a similar manner to the eaves joint as shown in Fig. 13. Validation of the

Table 7 Rotational stiffness of bolt-group for various arrays of bolts

| Number of bolts | $k_B$ |
|---|---|
| 2 × 2 = 4 | $(a_B^2 + b_B^2)k_b$ |
| 3 × 3 = 9 | $\frac{3}{2}(a_B^2 + b_B^2)k_b$ |
| 4 × 4 = 16 | $\frac{20}{9}(a_B^2 + b_B^2)k_b$ |
| 5 × 5 = 25 | $\frac{25}{8}(a_B^2 + b_B^2)k_b$ |

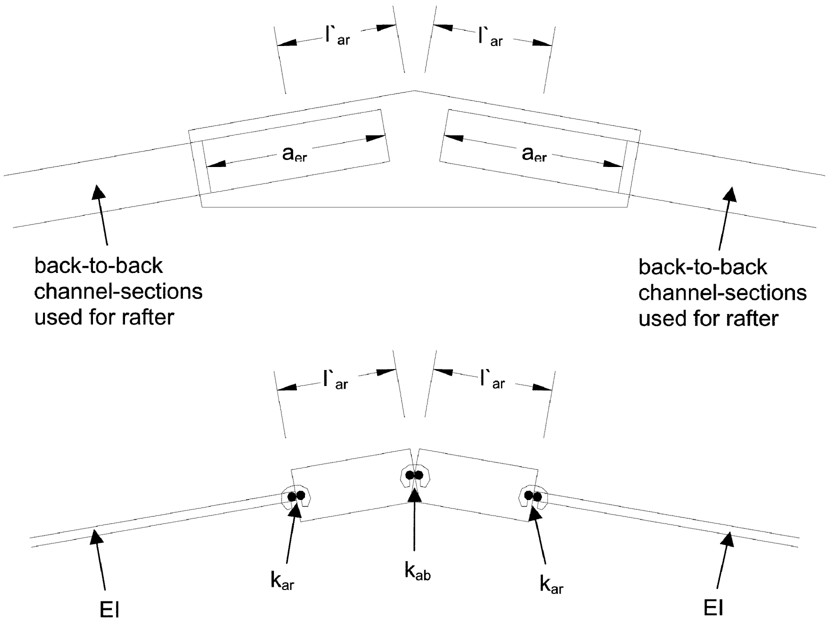


Fig. 13 Beam idealisation of apex joint

Table 8 Parameters pertaining to Frames A and B in analysis using beam idealisation

| Frame | $l'_{er}$ (mm) | $l'_{ec}$ (mm) | $l'_{ar}$ (mm) | $k_{ec}\times10^{-3}$ (kN.m/rad) | $k_{er}\times10^{-3}$ (kN.m/rad) | $k_{ar}\times10^{-3}$ (kN.m/rad) |
|---|---|---|---|---|---|---|
| A | 400.1 | 400.1 | 287.5 | 2.4 | 2.4 | 2.4 |
| B | 550.1 | 550.1 | 446.5 | 6.8 | 6.8 | 6.8 |

beam idealisation of the portal frame described can be found in Lim (2001) where the deflections are compared to those obtained using a shell idealisation.

The parameters pertaining to Frames A and B in the analysis using the beam idealisation are given in Table 8.

## *7.2. Comparison with serviceability requirements*

Table 10 shows the deflections of Frames A and B for a bay spacing of 6.37 m. It can be seen from Table 10 that while the eaves deflection limits are satisfied by Frame A, the apex deflection limit is not.

Table 9 Non-dimensionalised parameters pertaining to Frames A and B in parametric study

| Frame | Eaves joint | | Apex joint | |
|---|---|---|---|---|
| | $L_j$ | $K_j$ | $L_j$ | $K_j$ |
| A | 0.033 | 1.28 | 0.024 | 1.28 |
| B | 0.049 | 3.65 | 0.037 | 3.65 |

Table 10 Comparison of calculated serviceability deflections with suggested limits for Frames A and B having $b_f = 6.37$ m

| | | | Frame A | | Frame B | |
|---|---|---|---|---|---|---|
| Deflection category | Deflection limit | Deflection limit for frame (mm) | Calculated deflection for frame under SLC1 (mm) | Calculated deflection for frame under SLC2 (mm) | Calculated deflection for frame under SLC1 (mm) | Calculated deflection for frame under SLC2 (mm) |
| Lateral eaves deflection | $h_f$ / 100 | 30.0 | 18.9 | 17.69 | 7.4 | 5.4 |
| | $h_f$ / 150 | 20.0 | | | | |
| Vertical apex deflection | $\sqrt{b_f^2 + s_f^2}/125$ | 50.0 | 108.1 | 77.4 | 42.8 | 30.4 |
| | $L_f/240$ | 70.0 | | | | |

Note: The deflections shown above for SLC1 and SLC2 are in opposite directions

Therefore, Frame A cannot be designed to have a bay spacing of 6.37 m. In fact to satisfy serviceability requirements, the maximum bay spacing allowed for Frame A can be easily calculated to be 2.95 m.

On the other hand, it can be seen from Table 10 that both eaves and apex deflection limits are satisfied by Frame B. No reduction in bay spacing is therefore required and a bay spacing of 6.37 m (or more) can be used for Frame B. It can therefore be concluded that Frame B having semi-rigid joints, is as efficient as a rigid-jointed frame. The feasibility of a cold-formed steel portal frame having semi-rigid joints has therefore been demonstrated.

It can also be seen from Table 10 that the apex deflection under SLC1 is the most critical deflection. In other words, if the frame satisfies the critical apex deflection under SLC1, then all other deflection limits under both SLC1 and SLC2 are also satisfied. It can also be seen from Table 10 that for both SLC1 and SLC2, the eaves deflection is much less critical than the apex deflection.

## 8. Effects of semi-rigid joints and finite connection-lengths on behaviour of portal frames

In this Section, the beam idealisation will be used in a parametric study to demonstrate the effects of semi-rigid joints and finite connection-lengths on the deflections of the cold-formed steel portal frame. Two types of loading are considered: a vertical load case and a wind load case, referred to as wind load combination 1 (WLC1) in Section 5.

### 8.1. Details of frame used in parametric study

The standard portal frame of Fig. 5 will again be used for the parametric study. Fig. 14 shows details of the semi-rigid joints of finite connection-length. As can be seen, all the connections have been

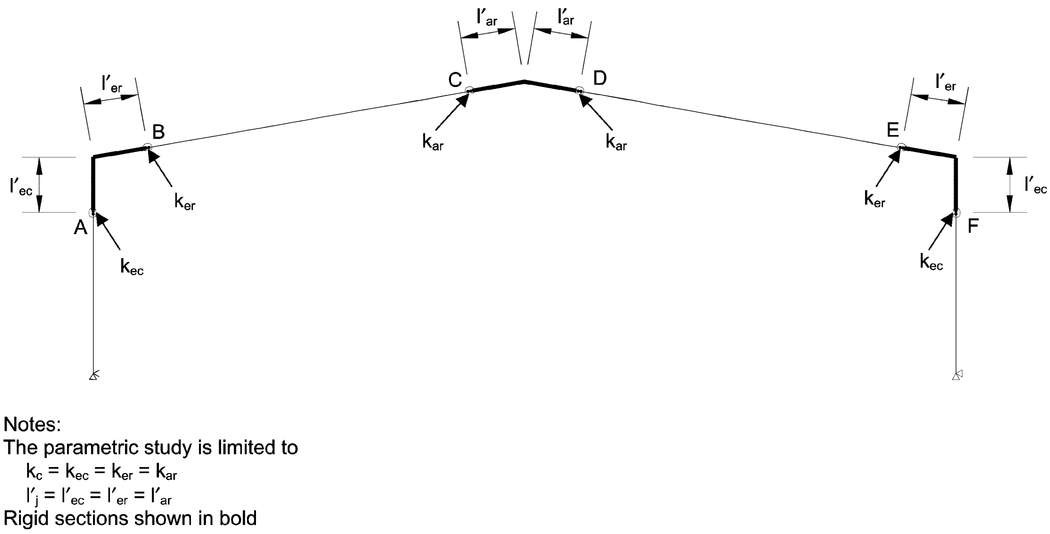


Fig. 14 Details of standard portal frame used in parametric study showing semi-rigid joints of finite connection-length

assumed to have the same rotational stiffness $k_c$ and the same connection-length $l_j'$.

Two non-dimensionalised parameters will be considered in the parametric study. Firstly, the joint rotational stiffness coefficient $K_j$ defined as

$$K_j = \frac{k_j}{EI/L_f}$$

where

$k_j$ = joint rotational stiffness
$EI$ = flexural rigidity of column or rafter member
$L_f$ = span of portal frame

As the connections are in series at each joint, $k_j$ is equal to half of $k_c$. The definition of the joint rotational stiffness ratio ($K_j$) is consistent with the EC3 (1996) definition used for classifying joints as rigid, semi-rigid, or nominally pinned. Under the EC3 classification system, a rigid joint is assumed to have a value of $K_j$ greater than 25, while a semi-rigid joint has a value of $K_j$ between 0.5 and 25.

Secondly, the connection-length coefficient $L_j$ defined as

$$L_j = \frac{l_j'}{L_f}$$

where

$l_j'$ = joint connection-length

The portal frame will be analysed elastically using six different values of $K_j$ (0.5 to 25.0) and ten different values of $L_j$ (0.01 to 0.10).

The deflections and bending moments obtained from the analysis of the frame considered here are non-dimensionalised by dividing them by the corresponding deflections and bending moments obtained from the analysis of the portal frame for which rigid connections and zero connection-lengths were assumed (see Section 6).

### 8.2. Deflection under vertical load

Fig. 15 shows the variation of the horizontal deflection at the eaves and the vertical deflection at the apex for a frame subject to vertical load against $L_j$ for various values of $K_j$. It is not surprising that both graphs are similar as there is a simple geometrical relationship between the vertical deflection at the apex and the horizontal deflection at the eaves for frames under vertical load.

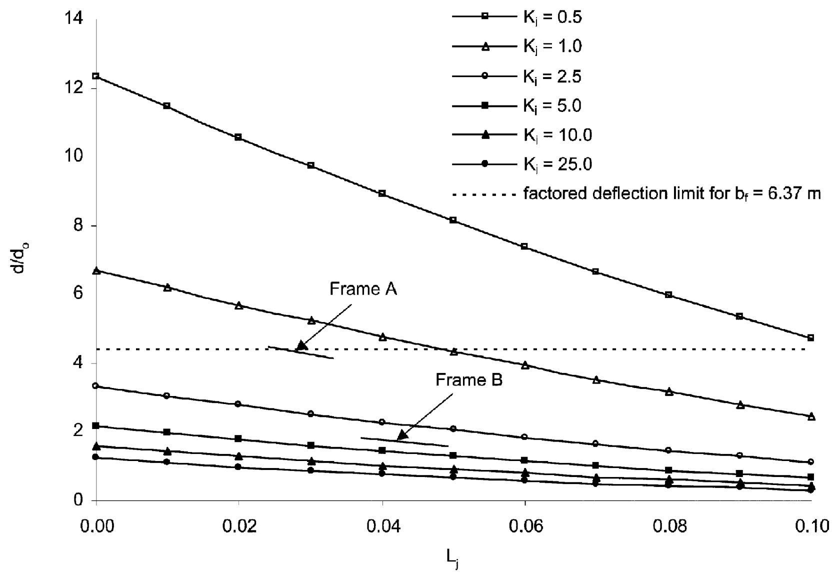


(a) Horizontal deflection ratio at eaves

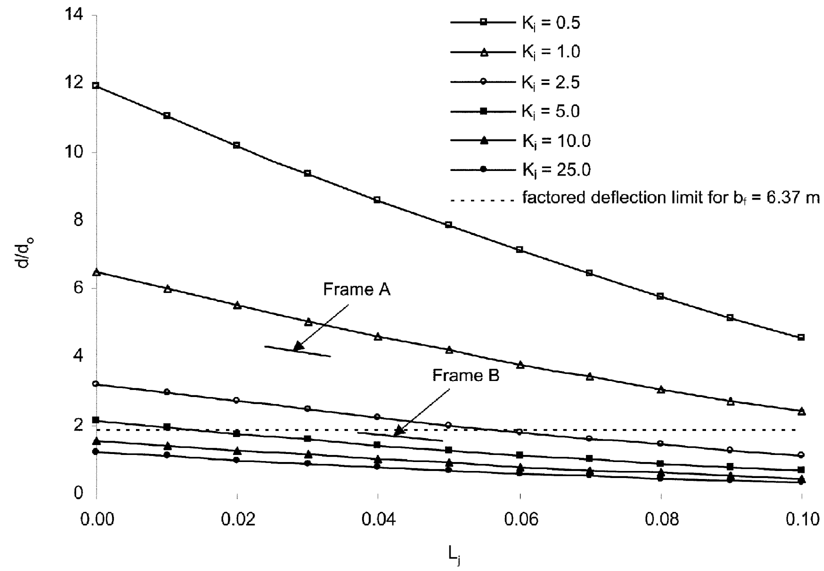


(b) Vertical deflection ratio at apex

Fig. 15 Variation of deflection against connection-length for various values of joint rotational stiffness for standard frame under vertical load

From Fig. 15 it can be seen that the frame deflections decrease almost linearly with $L_j$. A frame with joints having a value of $K_j$ of 0.5 and zero connection-length has deflections that are 12.3 times larger than that of a rigid frame. The effect of increasing $L_j$ to 0.1 reduces the deflection to approximately 4.7 times that of a rigid frame. On the other hand, a frame with a value of $K_j$ of 25 and zero connection-length has a deflection that is approximately 1.2 times that of a rigid frame. The effect of increasing $L_j$ to 0.1 reduces the deflection to approximately 0.3 times that of a rigid frame.

It can also be seen that the effect on deflections of increasing values of $K_j$ is larger for joints with lower values of $K_j$. For example, for the range of $L_j$ under consideration, doubling the value of $K_j$ from 0.5 to 1.0 reduces deflections by 45% while doubling $K_j$ from 12.5 to 25.0 reduces deflections by only 14%.

From Fig. 15 it can be seen that connection-length should not be neglected in the analysis of cold-formed steel portal frames having the joints described; in some cases connection-length can have as significant an effect as joint rotational stiffness on frame deflections.

### *8.3. Deflection under wind load*

Fig. 16 shows the variation of $K_j$ and $L_j$ on the vertical deflection at the apex for a frame subject to wind load combination 1 (WLC1). For the sake of brevity, only the vertical deflection at the apex has been shown as this was found to be more critical than the horizontal eaves deflection in the previous Section.

It can be seen that Fig. 16 is very similar to Fig. 15. The comments on connection-length made in the previous sub-section for vertical load also apply here for wind load.

### *8.4. Applications of deflection curves to Frames A and B*

It will now be shown how the deflection curves given as Fig. 15 and Fig. 16 can be used to predict the values of deflection for Frames A and B described in the previous sub-section.

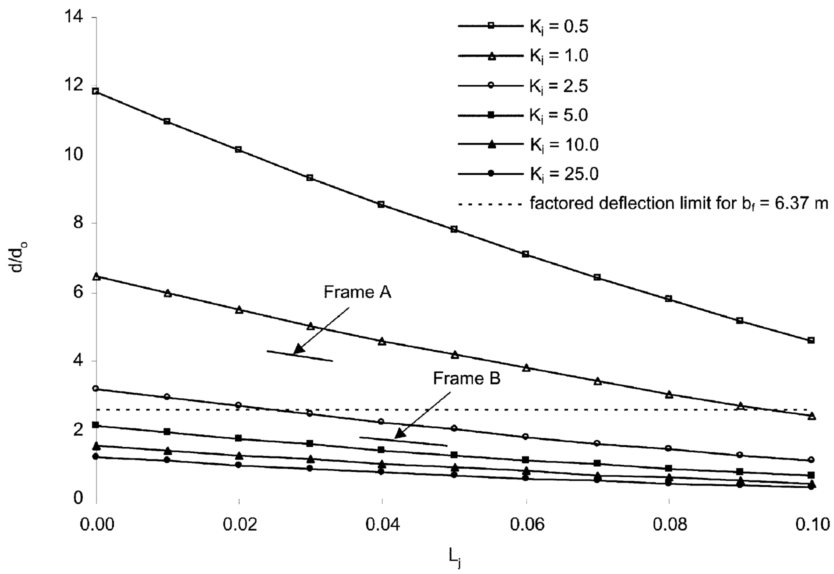


Fig. 16 Variation of apex deflection against connection-length for various values of joint rotational stiffness of joint for standard frame under wind load combination 1 (WLC1)

The parameters required to model both Frames A and B using the beam idealisation were given in Table 8. Table 9 shows these same parameters expressed in terms of $K_j$ and $L_j$. From this table it can be seen that the value of $K_j$ for both the eaves and apex joints of each frame is the same. This is because the eaves and apex joints of each frame are formed using the same bolt-group size and number of bolts. On the other hand, the value of $L_j$ is different for the eaves and apex joints of each frame owing to the different shapes of the eaves and apex brackets.

However, in the parametric study it was assumed that both the eaves and apex joints have the same value of $L_j$. Therefore, as the value of $L_j$ is different for the eaves and apex joints for Frames A and B, Fig. 15 and Fig. 16 cannot be used to interpolate the deflections directly.

Instead, it can be said that the deflections of Frame A will lie between that of a frame with $K_j$ of 1.28 and $L_j$ of 0.033, and that of a second frame with $K_j$ of 1.28 and $L_j$ of 0.024. Similarly, the deflections of Frame B will lie between that of a frame with $K_j$ of 3.65 and $L_j$ of 0.049, and a second frame with $K_j$ of 3.65 and $L_j$ of 0.037. Table 11 shows the deflection ratios interpolated from Fig. 15 and Fig. 16 for these values of $K_j$ and $L_j$. As a matter of interest, the results of an exact analysis of Frames A and B, in which different values of $L_j$ are used for the eaves and apex joints, are also shown in Table 11.

Using the results of the exact analysis (although in practice the deflections would be estimated from the two limiting cases), Frames A and B will be checked to determine whether the eaves and apex deflections satisfy the deflection limits under both serviceability load combination 1 (SLC1) and serviceability load combination 2 (SLC2) as described in Section 5. For both frames, it should be remembered that the bay spacing of the rigid frame of 6.37 m has been assumed.

As explained previously, Frames A and B cannot be shown directly in Fig. 15 and Fig. 16 because the eaves and apex joints have different values of $L_j$. Instead, the limiting values between which the deflections of Frames A and B will lie are shown in Fig. 15 and Fig. 16.

The dotted lines shown in Fig. 15 and Fig. 16 indicate the deflection limits of a frame with a bay spacing of 6.37 m. The position of the dotted line in each figure is calculated from the ratio of the deflection limit to the deflections of a rigid frame (see Table 6). For example, the position of the dotted line shown in Fig. 15(a) is found by dividing 20.0 mm by 4.5 mm to give 4.44. In other words, if the horizontal deflection at the eaves of a frame is 4.44 times greater than that of a rigid frame, the frame will not satisfy the horizontal deflection limit imposed at the eaves.

Therefore, frames with deflections that lie below the dotted line can be designed to have a bay spacing equal to that of a rigid frame. On the other hand, frames with deflections that lie above the dotted line will require a reduced bay spacing.

Table 11 Deflection ratio for Frames A and B

| Frame | $K_j$ | $L_j$ for | | $d/d_o$ for | | |
|---|---|---|---|---|---|---|
| | | Eaves joint | Apex joint | Vertical load | | Wind load |
| | | | | eaves | apex | apex |
| A | 1.28 | 0.033 | 0.033 | 4.12 | 4.00 | 3.99 |
| | | 0.024 | 0.024 | 4.47 | 4.33 | 4.32 |
| | | 0.033 | 0.024 | 4.20 | 4.07 | 4.05 |
| B | 3.65 | 0.049 | 0.049 | 1.59 | 1.56 | 1.56 |
| | | 0.037 | 0.037 | 1.81 | 1.77 | 1.77 |
| | | 0.049 | 0.037 | 1.64 | 1.61 | 1.60 |

The relative positions of the dotted lines in Fig. 15 and Fig. 16 also demonstrate that the apex deflection under vertical load is the critical deflection.

It should be noted that Frame B has satisfied the deflection limits with a value of $K_j$ of 3.6 that is substantially different from a value of 25 of a rigid frame.

## 9. Deflection curves

In the previous Section, a parametric study of a portal frame was used to show the effect of different values of $K_j$ and $L_j$ on the deflections of the standard portal frame. It was shown that all three deflection curves are almost identical and that for a frame of span 12 m and height 3 m, the apex deflection under vertical load is the critical case.

The same deflection curves can be used for all portal frames of aspect ratio $L_f / h_f$ of 3 and pitch $10^o$. Using such a deflection curve, appropriate values of $K_j$ and $L_j$ can be determined and used to aid designers in designing suitable bolt-group sizes for the eaves and apex joints. However, it should be remembered that the dotted lines shown indicating the values are only valid for a frame of span 12 m and height 3 m under the loading defined in Section 7. For other frames of the same aspect ratio, the critical case and the position of the dotted lines will vary as these will also depend on the magnitude of the deflection limits and wind load.

Similar deflection curves to aid designers for portal frames of aspect ratio $L_f / h_f$ of 2 and 3 are shown in Fig. 17 and Fig. 18, respectively.

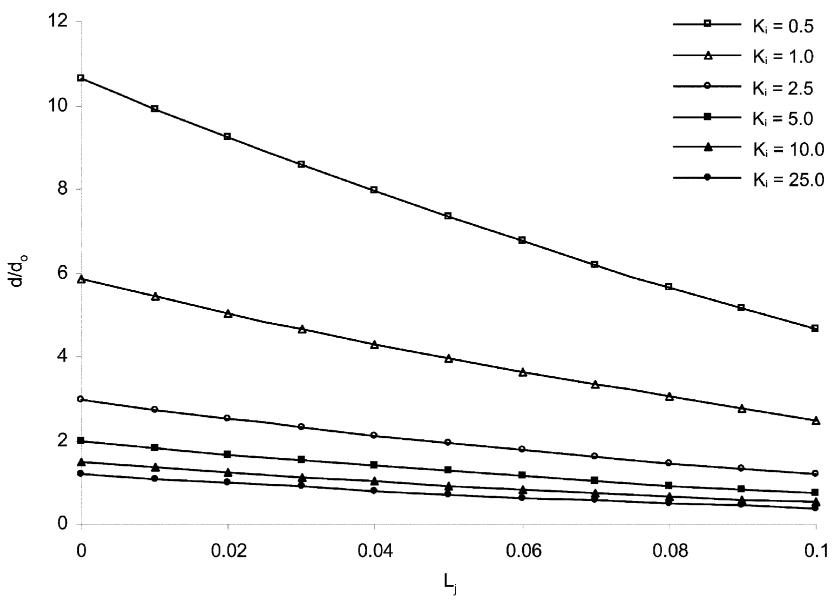


Fig. 17 Variation of critical apex deflection against connection-length for various values of joint rotational stiffness for frame of aspect ratio $L_f / h_f = 3$ under vertical load

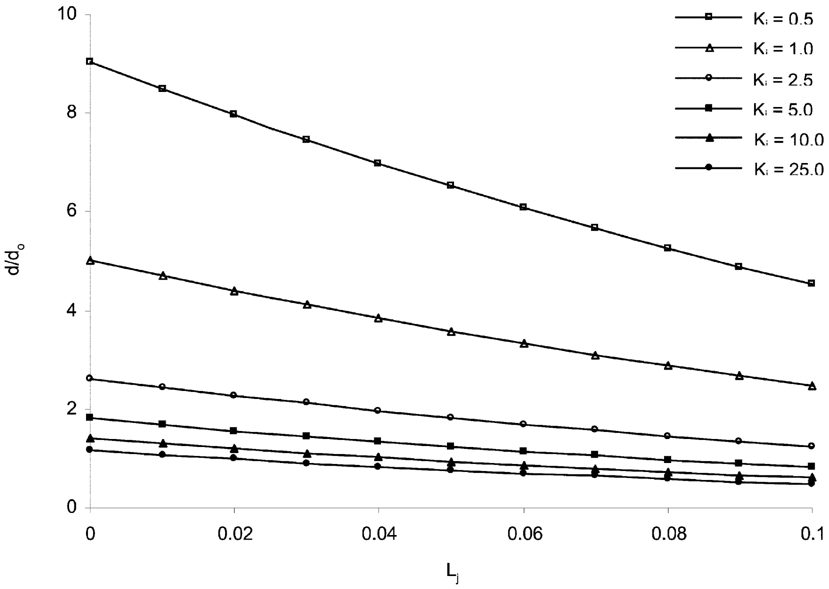


Fig. 18 Variation of critical apex deflection against connection-length for various values of joint rotational stiffness for frame of aspect ratio $L_f / h_f = 2$ under vertical load

## 10. Conclusions

The design of a cold-formed steel portal frame having semi-rigid joints has been described. Compared to rigid joints, semi-rigid joints are easy to fabricate and facilitate easy erection on site. Rational deflection limits have been defined for cold-formed steel portal frames and used to design a frame of span 12 m and height 3 m. Using the deflection limits, it has been demonstrated that for the cold-formed steel portal frame considered, semi-rigid joints are a feasible option to rigid joints. While frames of different spans and heights may result in designs that require substantially reduced bay spacings compared to rigid-jointed frames, it should be remembered that the cost of fabricating rigid joints must be taken into account when costing the frame.

Care must be taken in selecting joints of suitable rotational stiffness and size. To aid the designer, deflection curves for portal frames of three different aspect ratios have been provided.

## Acknowledgements

The work reported herein was undertaken in association with Ayrshire Metal Products as a “Partners in Technology” project with financial support from the DETR. The technical, financial and material contributions from Ayrshire are gratefully acknowledged. Thanks are also due to Mr. Thomas Cosgrove of the Steel Construction Institute for his technical discussions and comments.

## References

ANSYS, Inc. (1998), *User's Manual for Revision 5.5*, Pittsburgh, ANSYS, Inc.

Baigent, A.H. and Hancock, G.J. (1982), "The behaviour of portal frames composed of cold-formed members", *Thin-walled structures - Recent technical advances and trends in design, research and construction*, Oxford, Elsevier Applied Science, 209.

BS5950: Part 1 (2000), *Code of practice for design in simple and continuous construction: hot rolled sections*, London, British Standards Institution.

BS5950: Part 5 (1998), *Code of practice for design of cold-formed sections*, London, British Standards Institution.

Chung, K.F. and Ip, K.H. (2000), "Finite element modeling of bolted connections between cold-formed steel strips and hot-rolled steel plates under static shear loading", *Engng. Struct*, **22**, 1271.

CP3 (1972), *Code of basic data for the design of buildings: Chapter V: Part 2: Wind loads*, London, British Standards Institution.

De Vos, G.P. and Van Rensburg, B.W.J. (1997), "Lightweight cold-formed portal frames for developing countries", *Bldg Env.*, **32**(5), 417.

Eurocode 3 (1996), *Design of steel structures: Part 1 - General rules and rules for buildings*, Brussels, Committee European de Normalisation.

Kirk, P. (1986), "Design of a cold-formed section portal frame building system", *Proc. 8th International Speciality Conference on Cold-formed Steel Structures*, St. Louis, University of Missouri-Rolla, 295.

Lim, J.B.P. (2001), "Joint effects in cold-formed steel portal frames", University of Nottingham, PhD thesis.

Masika, R.J. and Dunai, L. (1995), "Behaviour of bolted end-plate portal frame joints", *J. Constr. Steel Res.*, **32**, 207.

Morris, L.J. and Plum, D.R. (1988), *Structural Steelwork Design to BS5950*, London, Longman Scientific and Technical.

SCI Advisory Desk (1991), "Deflection limits for pitched roof portal frames", *Steel Construction Today*, 203.

Woolcock, S.T. and Kitipornchai, S. (1986), "Portal frame deflections", *J. Aust. Inst. Steel Const.*, **20**(3).

## Notation

| | |
|---|---|
| $a_B$ | : length of bolt-group |
| $a_{ar}$ | : length of bolt-group pertaining to rafter to apex connection |
| $a_{ec}$ | : length of bolt-group pertaining to column to eaves connection |
| $a_{er}$ | : length of bolt-group pertaining to eaves to rafter connection |
| $b_B$ | : breadth of bolt-group |
| $b_{ar}$ | : breadth of bolt-group pertaining to rafter to apex connection |
| $b_{ec}$ | : breadth of bolt-group pertaining to column to eaves connection |
| $b_{er}$ | : breadth of bolt-group pertaining to eaves to rafter connection |
| $d$ | : deflection at eaves or apex |
| $d_o$ | : deflection at eaves or apex of rigid-jointed frame |
| $EI$ | : flexural rigidity of column and rafter members |
| $EA$ | : axial rigidity of column and rafter members |
| $h_f$ | : height to eaves of portal frame |
| $L_f$ | : span of portal frame |
| $b_f$ | : bay spacing between frames |
| $s_f$ | : length of rafter of portal frame |
| $\theta_f$ | : pitch of portal frame |
| $K_j$ | : $k_j$ non-dimensionalised by $EI/L$ |
| $k_j$ | : rotational stiffness of joints |
| $k_{ab}$ | : rotational stiffness of apex bracket |
| $k_{ar}$ | : rotational stiffness of rafter to apex connection |
| $k_{eb}$ | : rotational stiffness of eaves bracket |
| $k_{ec}$ | : rotational stiffness of column to eaves connection |

$k_{er}$ : rotational stiffness of rafter to eaves connection
$k_b$ : bolt-hole elongation stiffness
$l'_{ar}$ : effective length of bracket pertaining to rafter to apex connection
$l'_{ec}$ : effective length of bracket pertaining to column to eaves connection
$l'_{er}$ : effective length of bracket pertaining to rafter to eaves connection
$l'_j$ : effective length of joints
$L_j$ : $l'_j$ non-dimensionalised by $L_f$
$M_c$ : moment-capacity of back-to-back channel-sections used for column and rafter members

*CC*